Supplement of Atmos. Chem. Phys., 25, 4455–4475, 2025
https://doi.org/10.5194/acp-25-4455-2025-supplement

Atmospheric Chemistry and Physics
Open Access

Supplement of

Revisiting the high tropospheric ozone over southern Africa: role of biomass burning and anthropogenic emissions

Yufen Wang et al.

Correspondence to: Ke Li (keli@nuist.edu.cn)

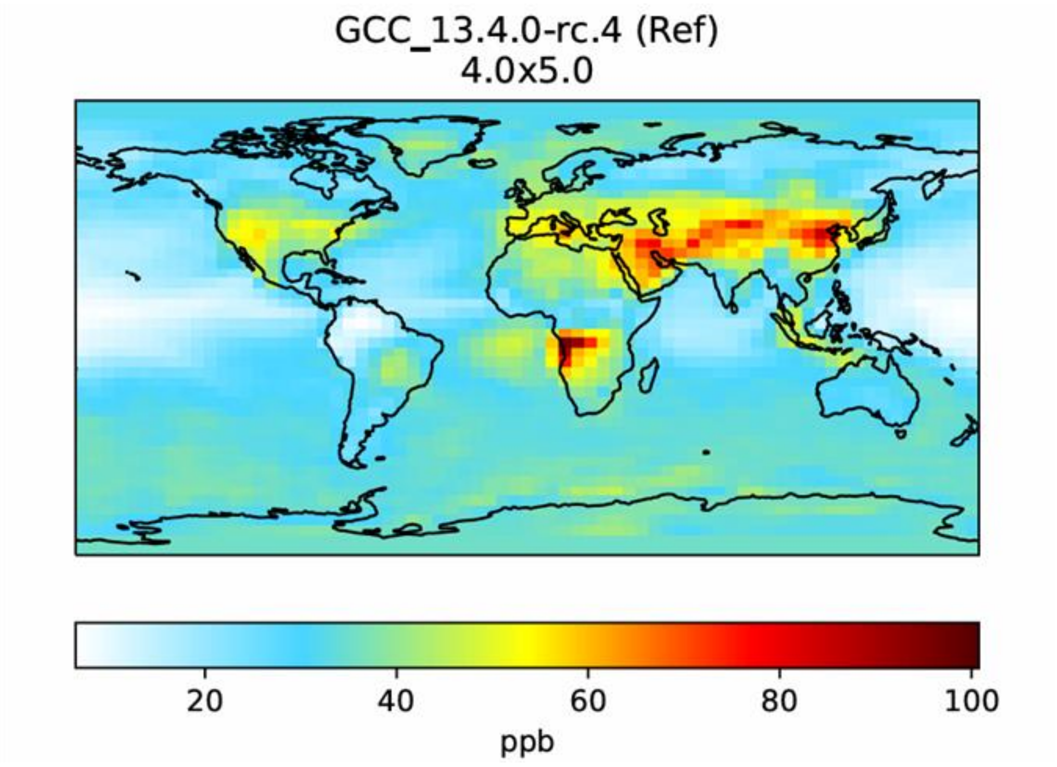

Figure S1. GEOS-Chem modelled surface ozone concentration obtained from the July 2019 benchmark experiment (downloaded from https://ftp.as.harvard.edu/gcgrid/geoschem/1mo_benchmarks/).

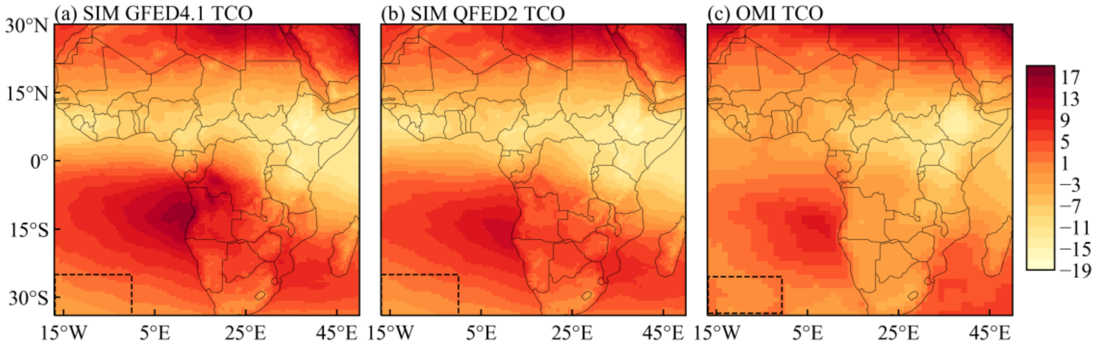

Figure S2. The comparison of GEOS-Chem simulated (left and middle panels) and satellite-based (right panel) tropospheric ozone columns after individually subtracting the background ozone values averaged over the black box (-34~-25 °S, 17 °W~0).

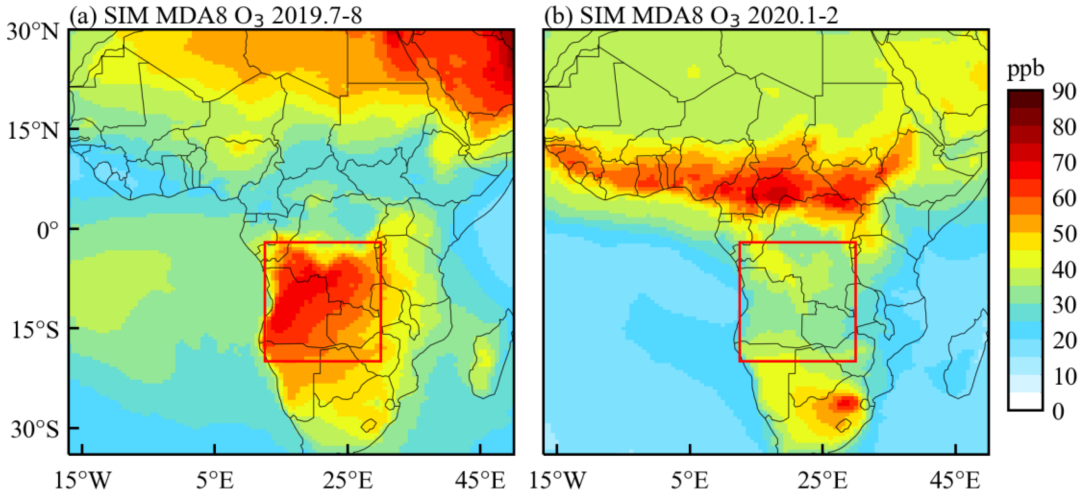

Figure S3. Spatial distribution of surface ozone during the fire season (July-August 2019) and non-fire season (January-February 2020) simulated by GEOS-Chem.

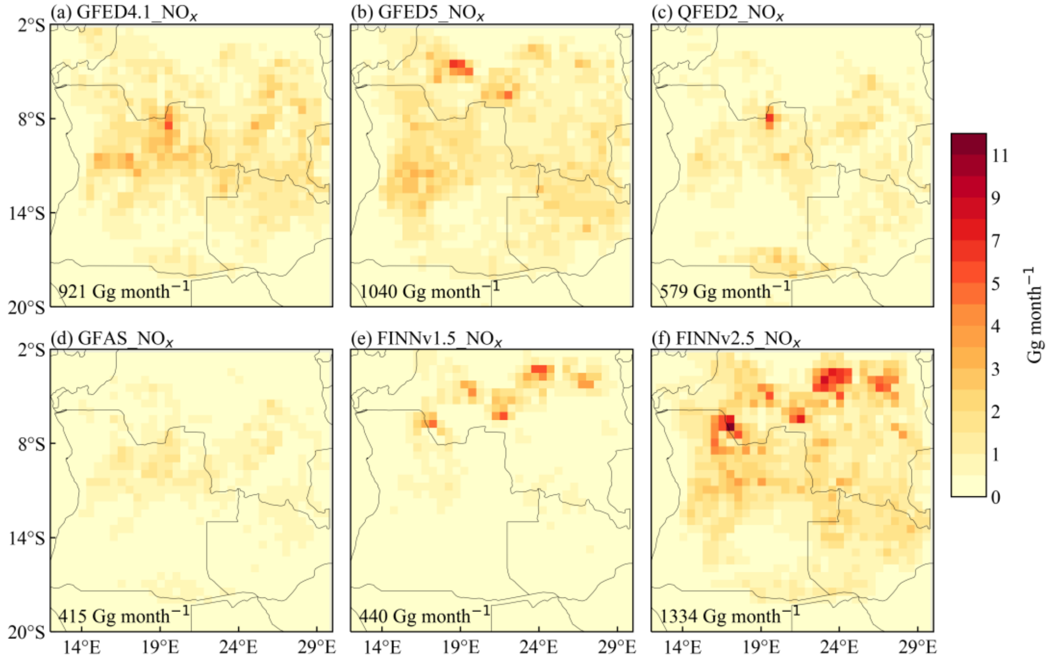

Figure S4. Spatial distribution of monthly NO_x emissions from different biomass burning emission inventories in July-August 2014.

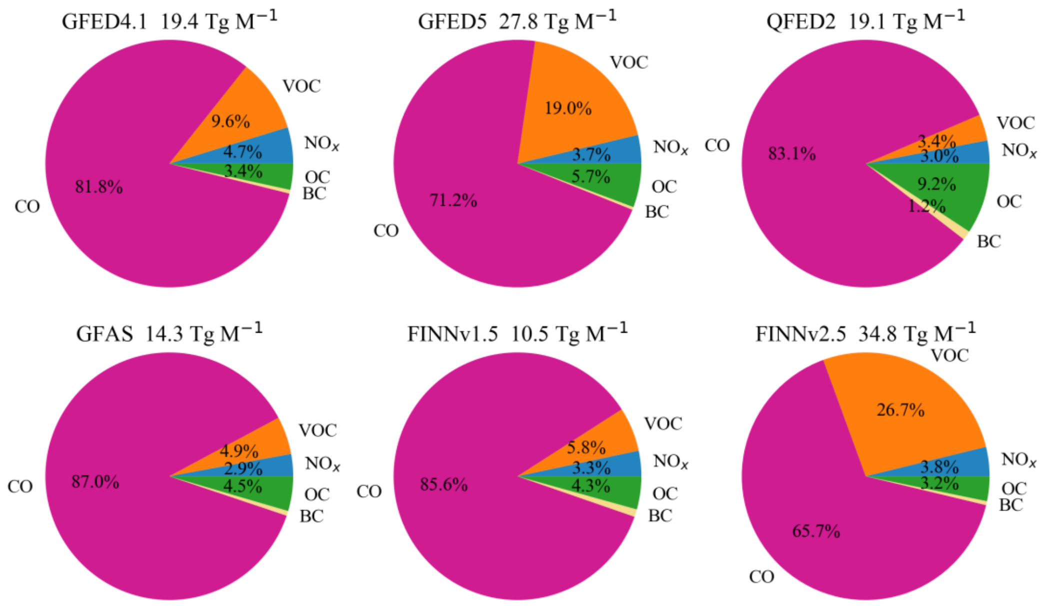

Figure S5. Estimated species emissions (Tg month^{-1}) in different biomass burning emission inventories in Southern Africa, July-August 2014.

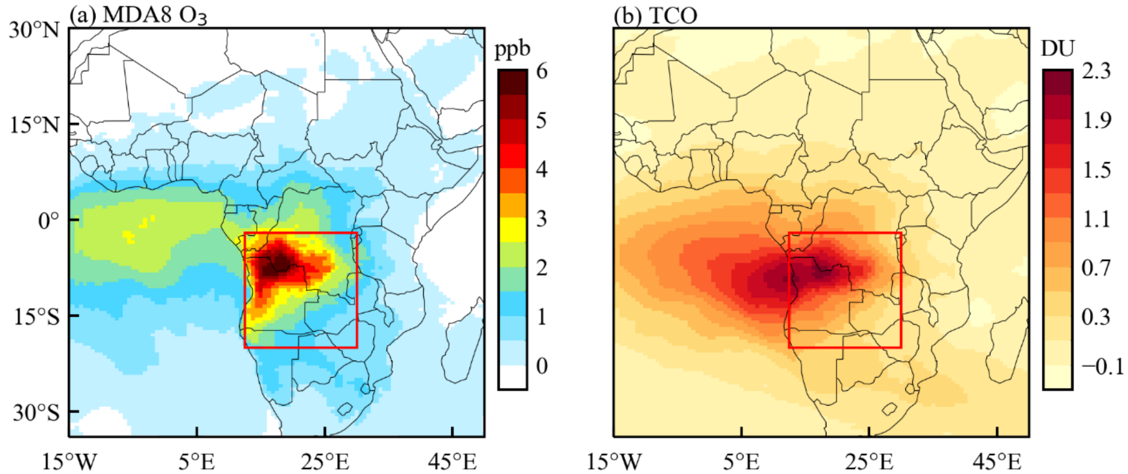

Figure S6. Changes in surface MDA8 ozone (left) and TCO (right) when VOC emissions from QFED2 inventories are tripled for July-August 2019. The regional mean changes are 2.5 ppb for MDA8 ozone and 0.94 DU for TCO.

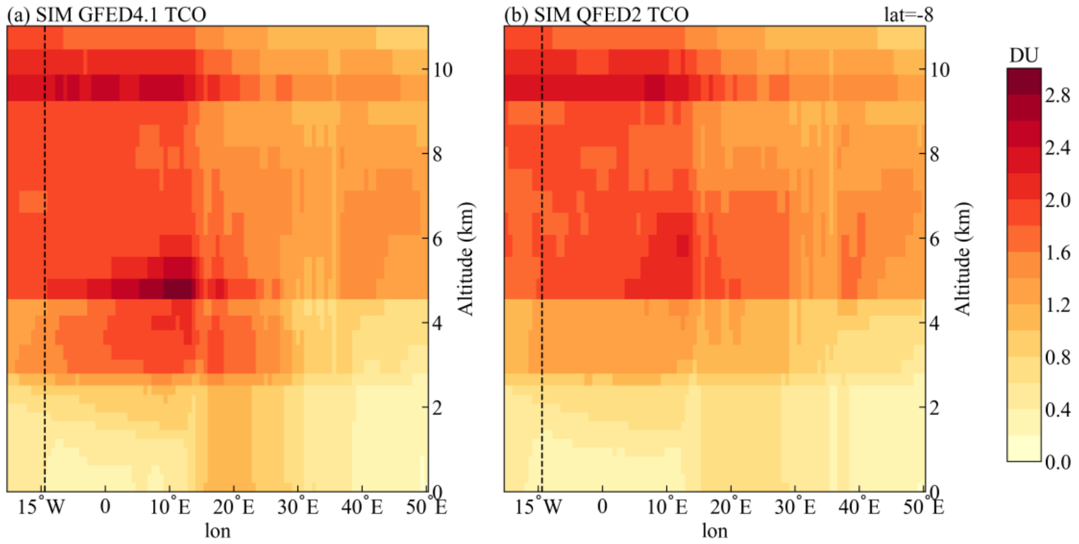

Figure S7. Vertical profiles of column concentrations across the latitude of -8°S simulated by GEOS-Chem using the GFED4.1 and QFED2 inventories, with the dashed line indicating the location of Ascension Island.

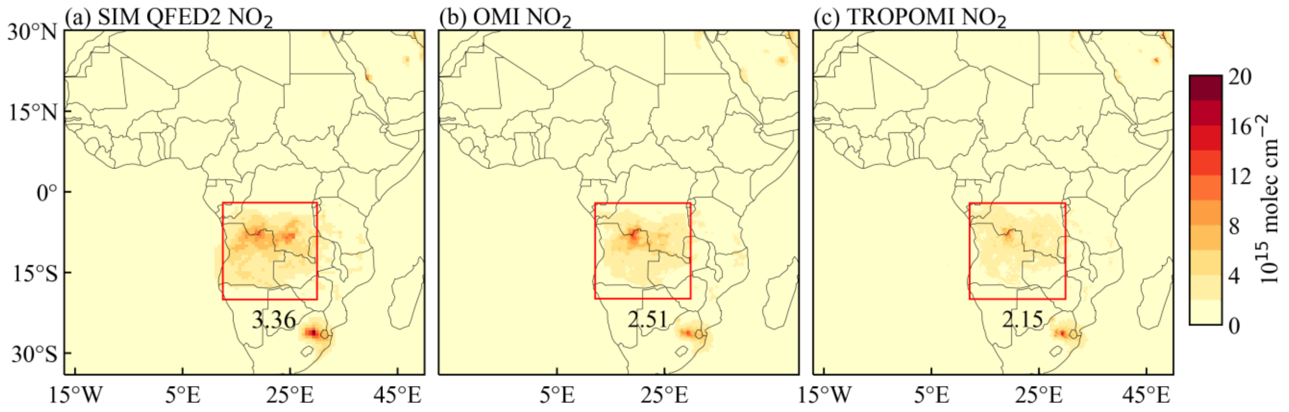

Figure S8. Comparison of the GEOS-Chem simulated NO_2 columns in Africa in July-August 2019 using the QFED2 inventory (a) with OMI (b) and TROPOMI (c). Numbers below the red boxes indicate the regional averages.

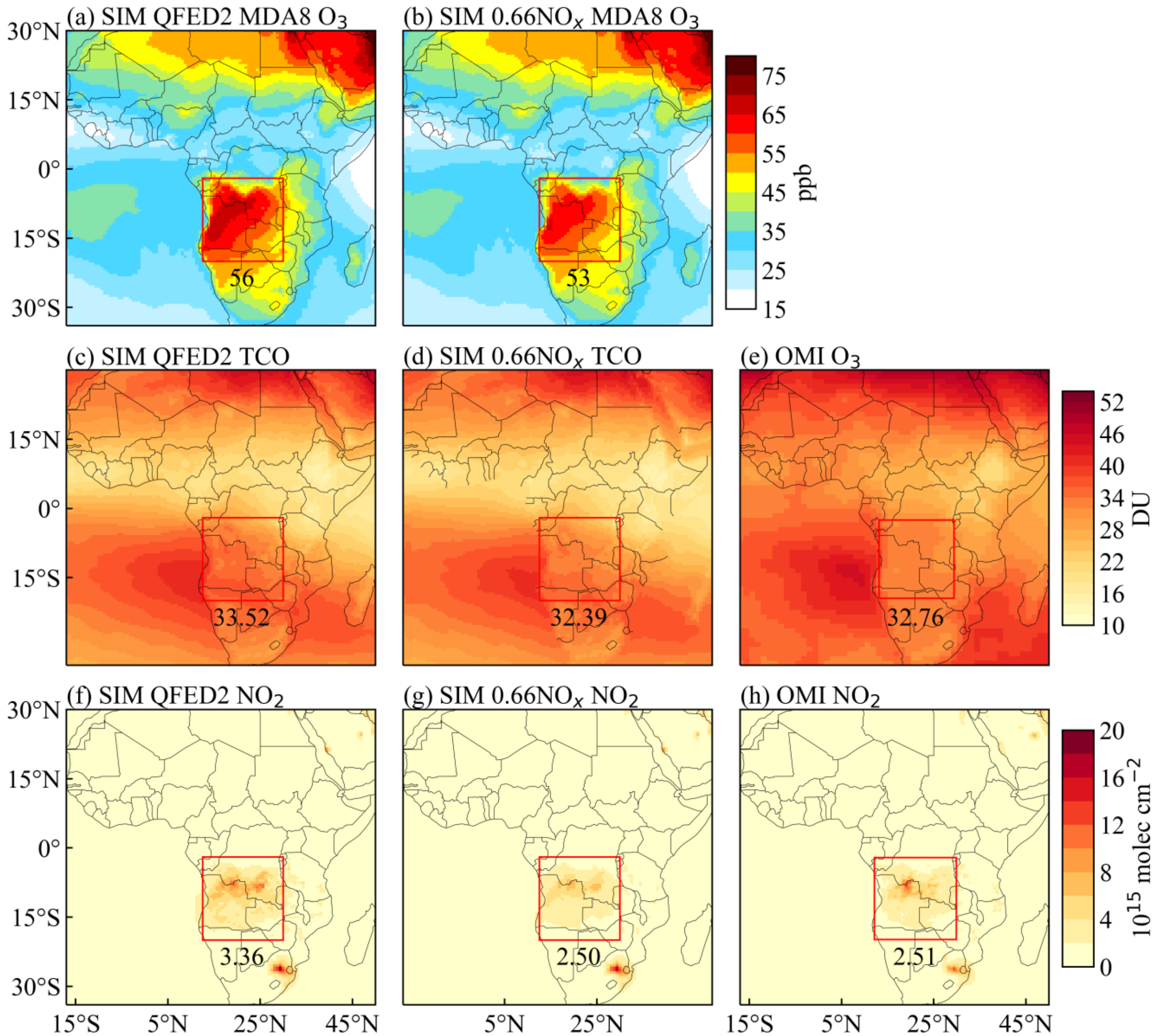

Figure S9. GEOS-Chem simulated surface ozone, tropospheric ozone columns, and NO_2 columns in Africa for July-August 2019 and its comparison with satellite data. The left panels are results from the baseline simulation; the middle panels are results from the simulation with 34% reduction in NO_x emissions from the QFED2 inventory; the right panels are results from the satellite data.

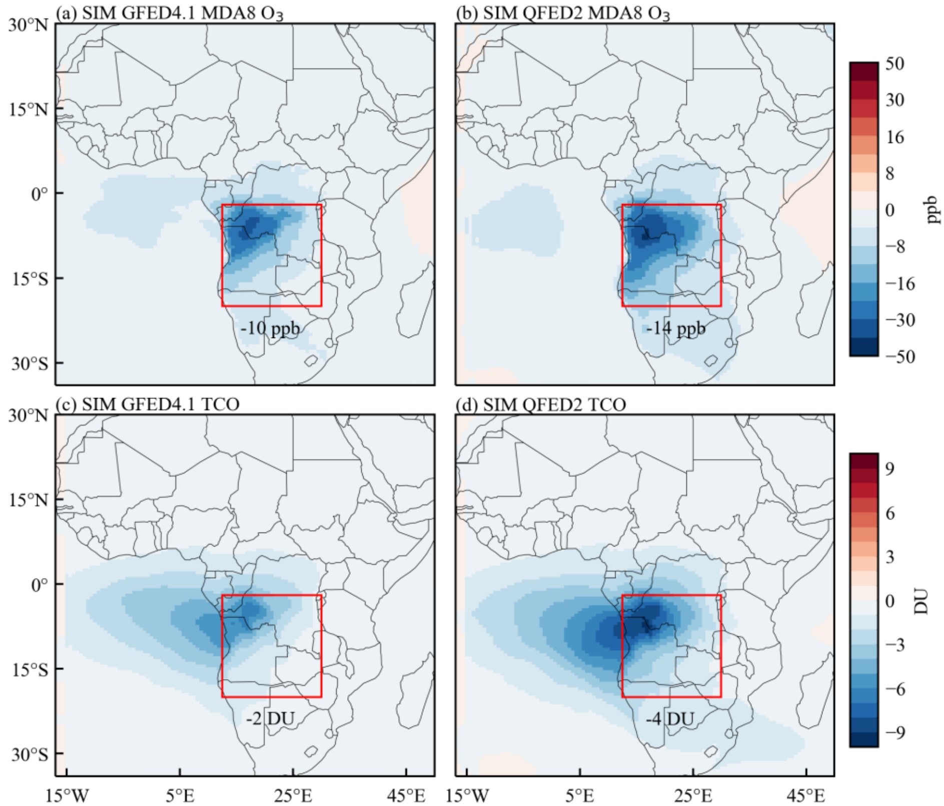

Figure S10. The simulated effects of aerosol chemistry on MDA8 ozone (top) and tropospheric ozone columns (bottom) in July-August 2019 by using the GFED4.1 and QFED2, respectively.

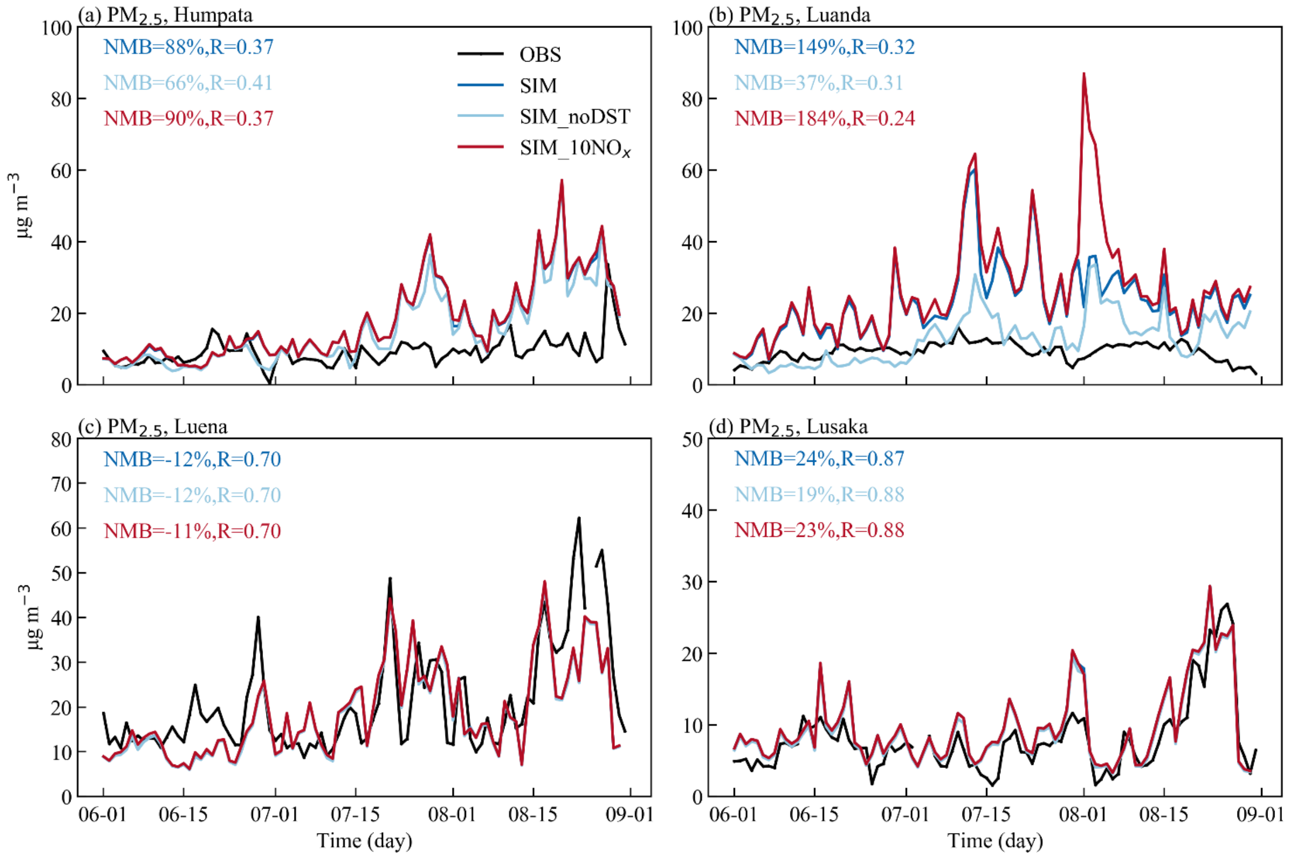

Figure S11. Time series of the simulated and observed (black) median daily $PM_{2.5}$ concentrations for June-August 2023. a-d are for Humpata, Luanda, Luena, and Lusaka, respectively. The plots labelled by the "SIM_noDST" and "SIM_10NO_x" are the $PM_{2.5}$ concentration after removing dust aerosols and the $PM_{2.5}$ concentrations when anthropogenic NO_x emissions were increased by a factor of 10 in CEDSv2.

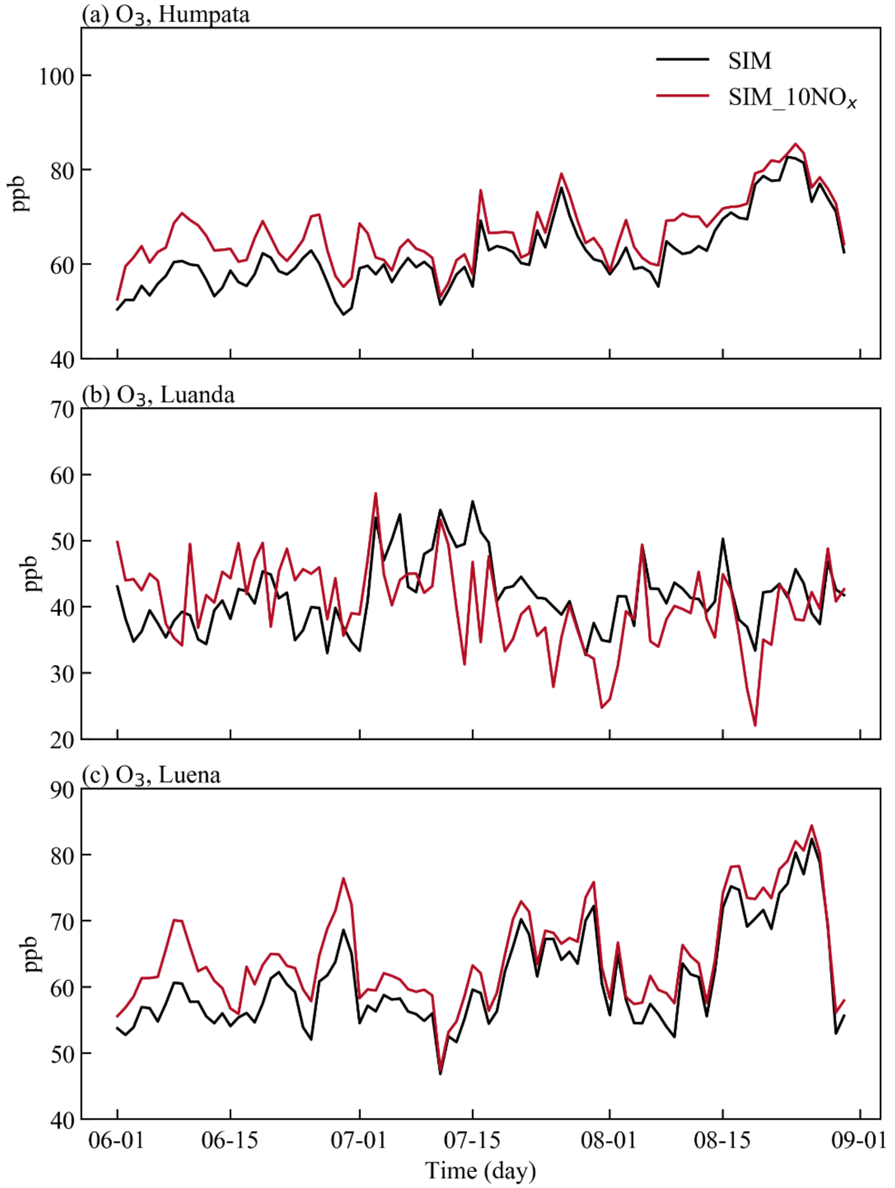

Figure S12. Time series of simulated June-August 2023 surface MDA8 ozone concentrations from the baseline simulation (black) and the sensitivity simulation (red) in which anthropogenic NO_x emissions were increased by a factor of 10 in CEDSv2.

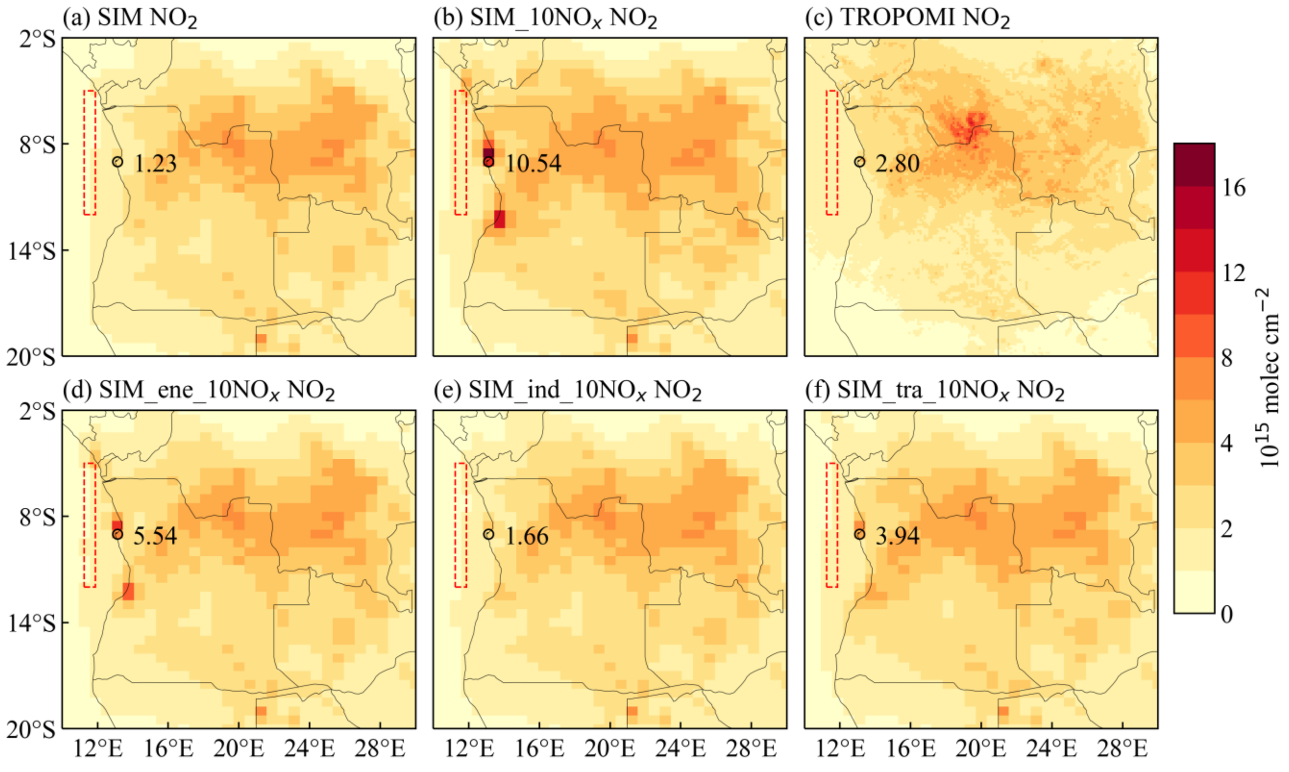

Figure S13. The observed and simulated tropospheric NO_2 columns in June-August 2023. (a) the baseline simulation with QFED2 inventory. (b) the sensitivity simulation with anthropogenic NO_x emissions increased by a factor of 10. (c) TROPOMI data. (d-f) the sensitivity simulations with sectoral NO_x emissions increased by a factor of 10 in energy, industry, and transportation. The numbers in the plots are all the relative NO_2 columns enhancement in Luanda area. The dashed boxes indicate the downwind background area, which is subtracted to obtain the relative NO_2 column concentration in Luanda.

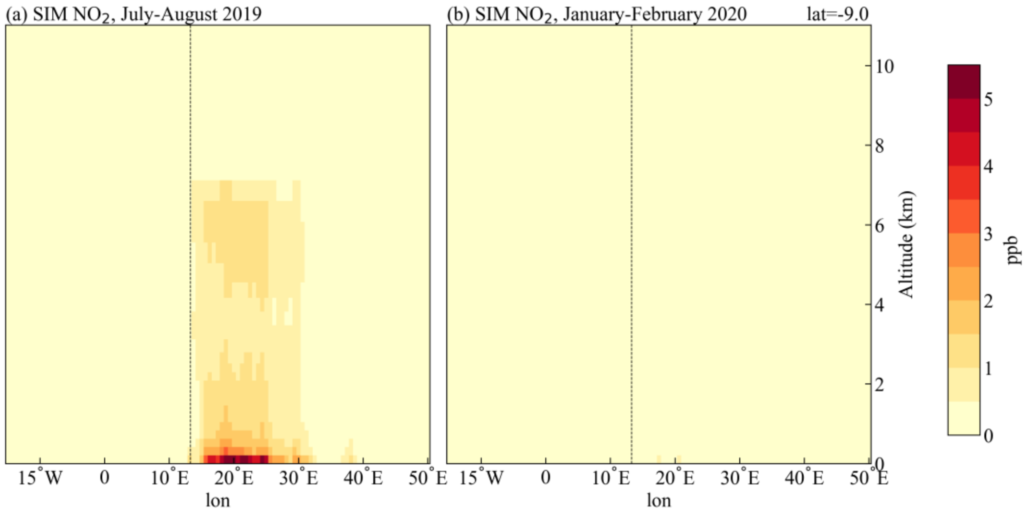

Figure S14. Vertical profiles of NO_2 across the latitude of -9 °S (Luanda is located at 8 °80'S, 13 °23'E) simulated by GEOS-Chem during the fire season (July-August 2019) and non-fire season (January-February 2020), with the dashed line indicating the location of Luanda.

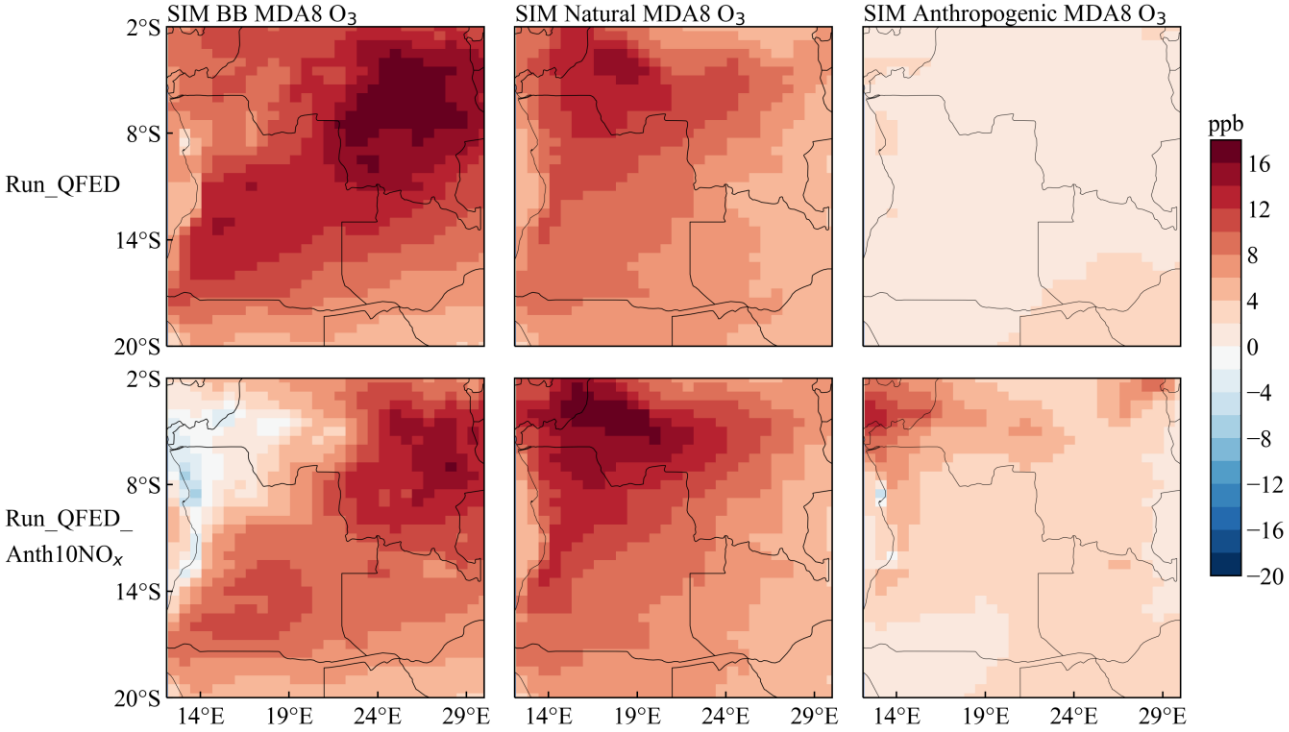

Figure S15. The simulated contributions to surface ozone in July-August 2019 from different sources, including biomass burning emissions (left), natural emissions (middle), and anthropogenic emissions (right), under Run_QFED simulation (top) and under Run_QFED_Anth10NO_x simulation (bottom) where anthropogenic NO_x sources were increased by a factor of 10. Here the natural emissions refer to the biogenic VOC and soil NO_x emissions.

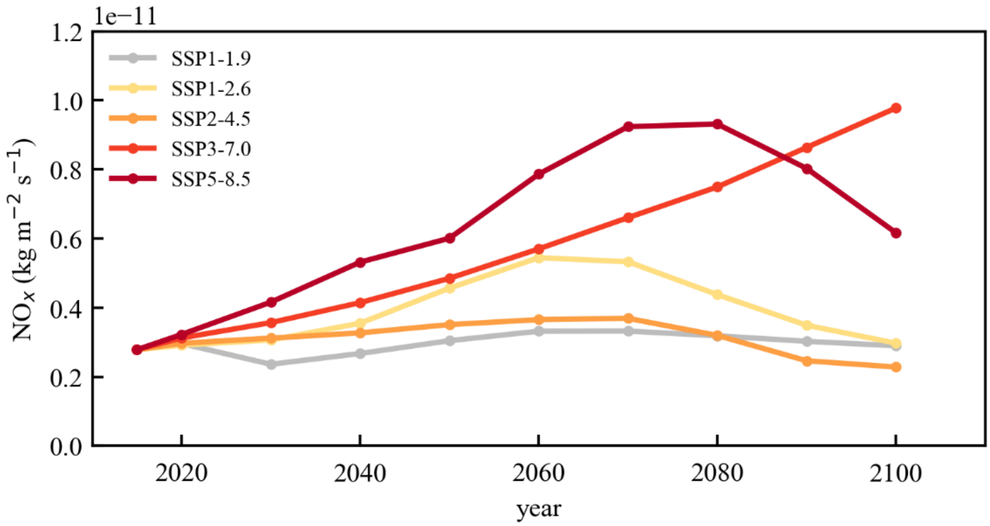

Figure S16. Trends in NO_x emission rates from anthropogenic sources under different future scenarios (Unit: kg m^{-2} s^{-1}).

Table S1. Statistics of spatial correlation coefficients between model simulation results and satellite data.

	GFED4.1		QFED2	
	NMB	R	NMB	R
OMI O_3	-10.4%	0.82	-12.9%	0.87
OMI NO_2	22.0%	0.83	9.3%	0.92
OMI HCHO	-2.9%	0.79	-5%	0.76
TROPOMI NO_2	8%	0.78	-3%	0.91
MODIS AOD	-34%	0.9	5.7%	0.89
MOPITT CO	-17.4%	0.89	-17.1%	0.89